IEEE Access
Multidisciplinary | Rapid Review | Open Access Journal

Received October 23, 2020, accepted November 14, 2020, date of publication November 17, 2020,
date of current version December 1, 2020.

Digital Object Identifier 10.1109/ACCESS.2020.3038759

A Radial Line Slot-Array Antenna With Low Side Lobes and a Uniform-Phase, Tapered-Amplitude Aperture Field Distribution

MST NISHAT YASMIN KOLI[1], (Graduate Student Member, IEEE), MUHAMAMD U. AFZAL[2], (Senior Member, IEEE), KARU P. ESSELLE[2], (Fellow, IEEE), AND RAHEEL M. HASHMI[1], (Member, IEEE)

[1]School of Engineering, Macquarie University, Sydney, NSW 2109, Australia
[2]School of Electrical and Data Engineering, University of Technology, Sydney, NSW 2007, Australia

Corresponding author: Mst Nishat Yasmin Koli (mst-nishat-yasmin.koli@students.mq.edu.au)

This work was supported in part by the International Macquarie University Research Excellence Scholarship (iMQRES) Scheme and in part by the Australian Research Council Discovery Grant.

ABSTRACT The paper presents a circularly polarized radial line slot array (CP RLSA) antenna with a nearly optimal monotonic variation of slot length with radius, in order to simultaneously reduce antenna side-lobe levels and to make the aperture phase distribution nearly uniform. It has additional advantages of excellent radiation efficiency, high gain and good overall bandwidth. The antenna comprises a single-layer radial transverse electromagnetic quasi-TEM waveguide with radiating slots on the aperture. The amplitude tapering is implemented by gradually varying slot lengths on the antenna aperture as a function of radial distance, utilizing a slot coupling analysis. Several antenna designs were investigated, each having a physical diameter of 345 mm ($23\lambda_0$) and a thickness of 4.6 mm ($0.3\lambda_0$), where λ_0 is the free-space wavelength at the operating frequency of 20 GHz. A prototype was fabricated and measured, showing a good agreement between the predicted and measured results. The sidelobe levels at the operating frequency are less than -20 dB due to tapering in the near-field amplitude distribution. The measured magnitude of the input reflection coefficient (S_{11}) of the antenna is below -10 dB within the frequency range of 19 GHz to 21 GHz. The antenna has a measured peak directivity and a peak gain of 34.3 dBic and 33.8 dBic, respectively. Both the measured 3dB directivity bandwidth and 3dB gain bandwidth are 5.4%. Aperture efficiency is 48% and radiation efficiency is 94.2% at the operating frequency. The fabricated antenna also successfully fulfilled the condition of circular polarization with an axial ratio bandwidth exceeding 5%.

INDEX TERMS Circularly polarized, CP, COTM, high gain, high efficiency, radial line slot array, LHCP, pattern quality, RLSA, RHCP, slot array, Beam steering, antenna, SATCOM, SOTM, slot array, side lobe level, SLL, 5G, 6G.

I. INTRODUCTION

A n unprecedented growth and dependency on wireless devices and components have steered a global effort to provide on-the-move connectivity to onboard mobile platforms using satellites and other high-altitude platforms. A key components of this communication model is an highly efficient front-end antenna system capable of steering its beam in a large angular range. Such beam-steering capability is essential when the satellite is not stationary relative to the communicating ground terminal.

Traditionally,the most widely used and low-cost solution for receiving satellite services such as satellite television (TV) is based on parabolic dishes. These parabolic dishes are affordable and efficient, but have serious constraints due to large volume when it comes to using on moving platforms such as a train or an aeroplane [1]–[4]. Furthermore, it is extremely challenging to swiftly track a satellite or re-align a parabolic dish to a satellite when the platform is moving. For these reasons only high-end solutions are available for

The associate editor coordinating the review of this manuscript and approving it for publication was Davide Comite.

on-the-move connectivity applications and low-cost reflector dishes are often used for stationary platforms.

RLSA antennas are considered one of the most attractive and versatile candidates as the base antenna for antenna beam steering systems based on Near-Field Meta-Steering [4]–[6] because of their promising features such as high gain, high efficiency, extremely low profile, and planar configuration [1], [7]–[19]. This paper presents an extremely high-gain radial-line slot array (RLSA) antenna that is useful as the base antenna in such systems. In order to address typical issues of side-lobes, the proposed CP RLSA base antenna has been designed with an optimal tapered amplitude distribution and a uniform phase distribution to maintain excellent far-field pattern quality. The novelty of the paper is the creation of an optimal amplitude taper in the antenna near field while maintaining a nearly uniform near-field phase distribution and by doing so, achieving significantly low side lobe levels in the far field while maintaining a high antenna gain and a large 3dB gain bandwidth.

The RLSA antennas are parallel plate waveguide antennas with a radiating slot pattern on the top plate and have been investigated in the past as an alternative to parabolic dishes [1], [2], [8], [20]–[26]. It is because of their extremely low height, they can conveniently be installed or even concealed on moving platforms. Several RLSA designs reported in literature focused on improving gain, efficiency and return loss performance [9], [23], [27]–[35]. On the other hand, a thorough investigation on RLSA side-lobe reduction methods is yet to be conducted [10], [36]–[44]. This paper addresses this need by developing a method that substantially reduces CP-RLSA side-lobe levels and at the same time enhances phase coherence across the aperture.

The aim of this paper is to develop a highly directive CP RLSA antenna that not only has extremely low sidelobes with excellent pattern quality but also has near-field radiation characteristics needed for beam steering applications. A strong emphasis has been, therefore, placed on achieving uniform aperture phase distribution along with optimally tapered amplitude field distribution on a plane parallel to the antenna aperture. A controlled amplitude distribution is achieved by manipulating the radiating slot lengths on the RLSA aperture, using a slot coupling analysis. Phase distribution is obtained by appropriately selecting the proper in-phase slot layout on the top radiating plate. The paper is arranged such that the operating principle and configuration of the antenna are explained in Section II. The analysis of electric near-field distributions and design examples are presented in Section III. Fabrication and measurement results are given in Section IV to validate the concept.

II. ANTENNA CONFIGURATION

The configuration of the CP RLSA antenna is shown in Fig. 1. It is made of two parallel conducting plates. The feed point is at the center of the bottom plate. These plates form a radial waveguide with radiating slots on its upper plate. The bottom plate behaves as a ground plane. The antenna is fed

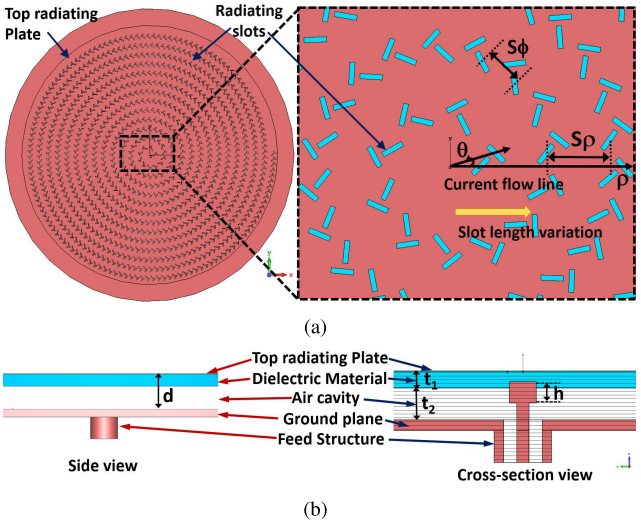

FIGURE 1. Configuration of the CP RLSA antenna (a) Layout of radiating slots on the top plate, (b) Side view and the cross-sectional view of the antenna.

at the center by a coaxial probe and it forms a rotationally symmetric outward travelling quasi-TEM wave in the radial waveguide. The slots are cut on the upper conductor and the power gradually radiates from these slots as the wave propagates from the center towards outer edge. The slots consist of many pairs; each one of which is a unit radiator that radiates a circular polarized electric field. The slots are arrayed along a spiral pattern to achieve constructive interference in the boresight direction. The spacings between adjacent slot pairs in radial and spiral directions are represented by S_ρ and S_ϕ, respectively, as shown in Fig. 1. To suppress the grating lobes, the waveguide is filled with a combination of dielectric material and air. The dielectric material filling the waveguide creates a slow wave and minimizes reflection towards the coaxial transmission line [2], [8]. An area of radius $\lambda_g/2$ around the center on the upper plate is left unslotted to allow the outward travelling wave to settle before radiating. When the height of the radial waveguide is limited to be less than one half guide wavelength, the only possible symmetric waveguide mode that can propagate within the radial waveguide is the TEM mode. The coaxial feed excites this mode within the radial waveguide. Electromagnetic power is fed from a coaxial transmission line into the center of the radial slow-wave waveguide by the feed probe. The feed has a disk head, shown in Fig. 1 (b), which converts the electromagnetic power from a TEM coaxial mode into a quasi-TEM radial waveguide.

The radiating plate, depending on aperture size, may have several hundreds of unit radiators, as shown in Fig. 1. A radiating unit consists of two slots that are placed orthogonally and have same length (L) and width, to radiate two orthogonal electric-field components with equal magnitude. To radiate circular polarization, the two slots in a unit radiator are physically separated by a distance of $\lambda_g/4$ in order to create a phase shift of 90°, where λ_g is the guided wavelength. The first slot in a radiating unit is oriented to an angle of 45° with respect to the current flow line (a line drawn from the center

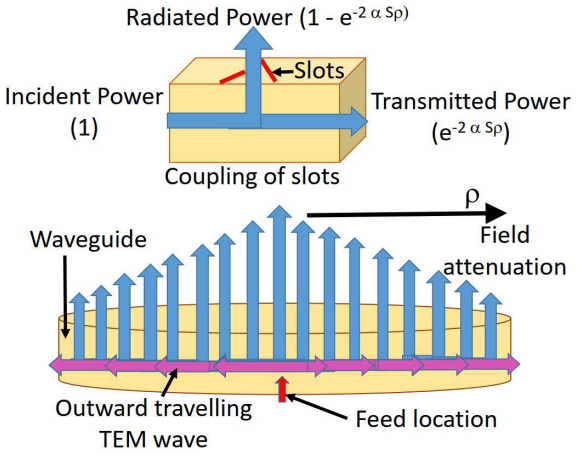

FIGURE 2. Coupling mechanism of radiating slots and attenuation of outward travelling wave.

of the radiating surface towards the edge), whereas the second slot in the radiating unit is oriented to an angle of $45° + \theta$, where θ is the angle between the two slots in a radiating unit. The RLSA aperture amplitude distribution is controlled by the lengths of radiating slots. A more detailed explanation of slot layout design of CP RLSA antennas is given in [7]. It was followed in this work.

A. SLOT COUPLING ANALYSIS

As the wave travels outwards in the radial waveguide, energy radiates through slot pairs. The reflections from the two slots in a unit radiator cancel each other as they are $\lambda_g/4$ distance apart and the internal field can be expressed as [19],

$$E = exp(-\alpha\rho - \frac{jk_0}{\zeta}\rho) \tag{1}$$

where α is the coupling coefficient, which represents internal field attenuation. The slow wave factor ζ indicates the wavelength reduction of the radially outward traveling wave due to slot coupling. Under the travelling wave operation, the incident power can be divided into slot radiation and transmitted power as pictorially represented in Fig. 2. The radiation from slots can be modeled as attenuation of internal power and can be written as $(1 - e^{-2\alpha S_\rho})$, and the transmitted power as $e^{-2\alpha S_\rho}$ [19]. If the attenuation due to slot radiation is higher in the middle of aperture, then the amplitude of the cylindrical wave and the aperture illumination will be steeply tapered. Therefore, slot coupling is the most important factor that controls the aperture field distributions of RLSAs, and consequently, the gains and far-field radiation patterns of RLSA antennas.

An RLSA antenna can be designed to produce a particular field distribution for lower sidelobes or higher aperture directivity. The field distribution of a circular planar antenna can be analytically expressed as [45],

$$A_n(\rho) = [1 - (\frac{\rho}{a})^2]^n;\ 0 \le \rho \le a,\ n = 0, 1, 2, 3 \ldots \tag{2}$$

where, ρ is the radial distance and a is radius of the circular aperture.

TABLE 1. Radiation characteristics of a circular aperture planar array [45].

Distribution	Uniform (n = 0)	Radial Taper (n = 1)	Radial Taper Squared (n = 2)
Analytical expression	$I_\circ[1-(\frac{\rho}{a})^2]^\circ$	$I_1[1-(\frac{\rho}{a})^2]^1$	$I_2[1-(\frac{\rho}{a})^2]^2$
Directivity factor	$(\frac{2\pi a}{\lambda})^2$	$0.75(\frac{2\pi a}{\lambda})^2$	$0.56(\frac{2\pi a}{\lambda})^2$
First sidelobe max.(dB)	-17.6	-24.6	-30.6
Half-power beamwidth (degrees)	$\frac{29.2}{a/\lambda}$	$\frac{36.4}{a/\lambda}$	$\frac{42.1}{a/\lambda}$

Equation (2) generates a uniform field distribution over the aperture when $n = 0$. As the value of n increases the distribution becomes tapered towards the edge. To achieve a specific objective, for example, radiation characteristics of the planar circular arrays with uniform and tapered field distributions are given in Table 1. From the Table 1, it can be seen that a uniform aperture distribution ($n = 0$) theoretically has highest directivity, whereas a radially taper squared aperture distribution ($n = 2$) leads to a lowest side lobe levels (SLLs) in circular planar arrays.

If all the unit radiators arrayed on the CP RLSA aperture have equal lengths and widths, then each slot couples almost a constant proportion of the radial power. As the power is fed at the centre of the CP RLSA, more energy will radiate from the slots close to the center and less energy will radiate from those closer to the edges. This will reduce the power intensity of the outward travelling quasi-TEM wave by a factor of $1/\sqrt{\rho}$ through the coupling of the radiating slots, which is not favourable in terms of boresight gain. Hence a proper slot coupling analysis is necessary to control illumination over the CP RLSA antenna aperture. One possible method is to keep the slot density constant ($S_\rho \times S_\phi = \text{constant}$) on the aperture and control the energy coupled by the unit radiators from the internal waveguide field to the radiating field.

This investigation is focused on creating a tapered amplitude distribution with proper slot coupling analysis for improving the radiation pattern quality by reducing the side lobe levels. The distribution is obtained by manipulating the slot lengths on the antenna aperture. The slot length can be written as a function of radial distance according to

$$L_{slot} = \delta + (\rho \times \alpha) \tag{3}$$

where δ is a constant factor that depends on the operating frequency, ρ is the radial distance, and α is the coupling coefficient, which is the rate at which the slot length increases with radius, i.e. $\partial L_{slot}/\partial\rho$. δ is optimised before creating the slot patterns. The term $(\rho \times \alpha)$ acts as a coupling factor. For a particular distribution, the coupling coefficient α needs to be optimised. As the radial distance increases, the coupling factor increases, leading to increasing slot lengths. By varying the slot lengths, we can control the proportion of energy

TABLE 2. Parameters of the antenna design.

Design Parameter	Value (mm)
Free-space wavelength (λ_0) (mm)	15
Equivalent waveguide permittivity (ϵ_r)	1.41
Guided wavelength (λ_g) (mm)	12.6 ($\lambda_0/\sqrt{\epsilon_r}$)
Aperture diameter (R) (mm)	345 ($23 * \lambda_0$)
δ (mm)	4.3
Slot width (mm)	1 ($\lambda_0/15$)
Slot depth (mm)	0.035
Number of rings, N	13
Waveguide height, d	4.575
Height of the dielectric material, t_1 (mm)	1.575
Dielectric constant of the dielectric material	2.2
Height of the air cavity, t_2 (mm)	3
Thickness of the disk-head , h (mm)	2
Adjacent slot-pair spacing along ρ direction (S_ρ) (mm)	12.6 (λ_g)
Adjacent slot-pair spacing along ϕ direction (S_ϕ) (mm)	7.5 ($\lambda_0/2$)
Initial radius (mm)	6 ($\lambda_g/2$)

coupled from the internal field to the radiating field, and hence the aperture taper.

III. INVESTIGATION ON NEAR-FIELD DISTRIBUTION

To investigate the influence of aperture field distribution on far-field performance, several CP RLSA antennas were designed. Different distributions were obtained by varying the slot length on the antenna aperture. Equation 3 was used to vary the slot lengths. The antennas were designed at 20 GHz following the design procedure explained in Section II and all of them have an aperture size of $23\lambda_0$ (345 mm). The common design parameters of the antennas are summarized in Table 2. All were designed to provide right hand circular polarization (RHCP). The spiral geometry is made with 13 rings of radiating slots. The waveguide was filled with Taconic TLY-5 dielectric material ($\epsilon_r = 2.2$) and air ($\epsilon_r = 1$). A 50 Ω disk ended feed probe was used to feed EM power at the center of the waveguide. The design parameters were kept constant for all the designs except the slot distribution on the top radiating plate. The slot layouts on the surface were created using a custom Visual Basic interface with CST Microwave Studio.

The plot of slot length (L_{slot}) as a function of radius is shown in Fig. 3 for five values of α. The value of δ is constant and set to an optimal value of 4.3. α is varied from 0.002 to 0.01 with a step size of 0.002. As it can be seen from the figure that as the value of α increases, the slot lengths increase. The near-field amplitude distributions and the far-field radiation patterns at 20 GHz for different values of α are shown in Fig. 4 (a) and Fig. 4 (b), respectively.

The electric near-field amplitudes of E_x are taken on a plane that is parallel to the XZ plane and located $1\lambda_0$ (15 mm) above the top radiating plate. As it can be seen from Fig. 4 (a), for $\alpha = 0.002$, the amplitude distribution is strongly tapered. As the value of α increases, the amplitude tapering weakens. Values of α in the range of 0.004 and 0.006 provide nearly a radial taper squared distributions, whereas α in the range

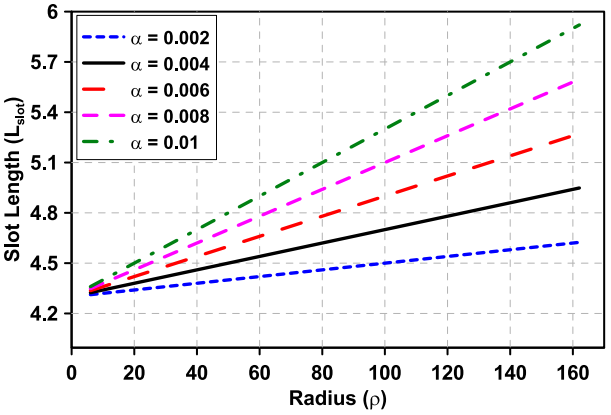

FIGURE 3. Variation of slot length (L_{slot}) with radius, for several value of coupling coefficient, α.

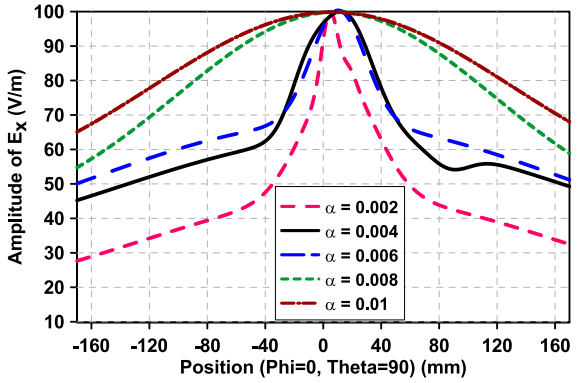

(a)

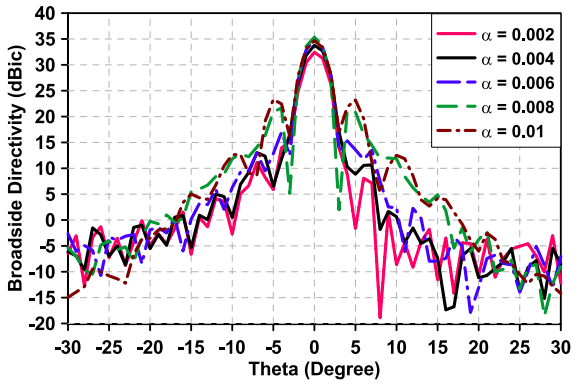

(b)

FIGURE 4. (a) Normalised electric near-field amplitude distribution for different values of α, (b) far-field radiation patterns for different values of α at 20 GHz.

of 0.008 and 0.01 provide nearly a radial taper amplitude distributions.

Table 3 summarises antenna performance figures for different values of α. The design with $\alpha = 0.002$ provides the lowest SLL of -21.3 dB. The SLL increases with the increase in α. On the other hand, far-field directivity increases with the increase in α. The electric near-field phase distributions for different values of α at 20 GHz are shown in Fig. 5. As it can be seen, α with a value of 0.004 makes a more uniform phase distribution than other values. For the selected value of

TABLE 3. Antenna performance for different rates at which slot length is increased with radius.

Rate α	Directivity	SLL ($\phi = 0°$)	3dB beamwidth	Aperture efficiency
	dBic	dB	Degrees	%
0.002	32.4	-21.3	2.6	28
0.004	33.8	-20.8	2.6	38
0.006	34.8	-17.8	2.5	49
0.008	35.4	-13.7	2.4	59
0.01	35.7	-11.4	2.4	64

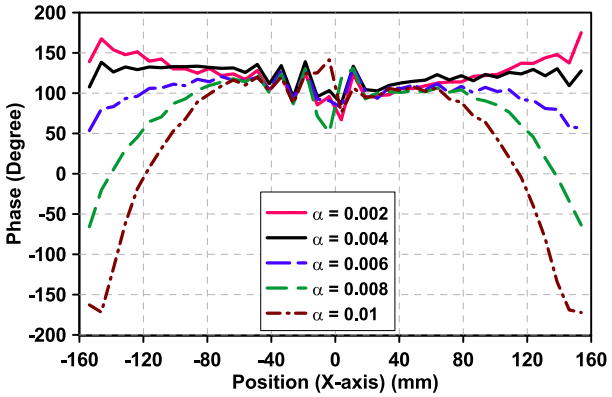

FIGURE 5. Electric near-field phase distribution for different values of α at 20 GHz.

α (= 0.004), the phase fluctuation throughout the aperture is only 45 degrees. Such a small phase variation is very much acceptable over the aperture and does not significantly affect radiation performance. Later, we have chosen this value of α for prototyped antenna design explained in the next section, as it provides a nearly uniform phase distribution and low side lobes.

IV. FABRICATION AND MEASUREMENTS

A. FABRICATED PROTOTYPE

One of the designs discussed above was fabricated to validate the concept. The parameters of the prototype are given in Table 2. The antenna was simulated using the time-domain solver of CST Microwave Studio to predict the near and far-field radiation characteristics. The front and back views of the fabricated prototype are illustrated in Fig. 6. The printed slot pattern was etched on a Taconic TLY-5 ($\epsilon_r = 2.2$) laminate. The slots were etched from a 0.035 mm thick copper cladding attached to the laminate. All slots have a width of 1 mm. Slot lengths vary as described above from 4.324 mm (inner slot) to 4.98 mm (outer slot). The ground plane is made with Aluminum. The Taconic TLY-5 laminate and bottom aluminum plate have holes around the edges. Nylon screws and spacers were used to hold the laminate with the Aluminium plate. The aluminum plate has a hole in the center for the 50 Ω coaxial connector. The connector has a disk-ended feed probe as shown in Fig. 6 (b). The disk head is 2 mm thick and 2.8 mm wide, made with Aluminum and glued on the top of the feed pin.

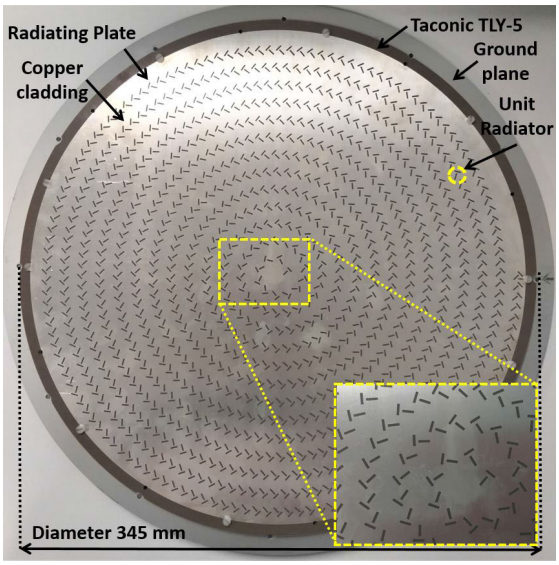

(a)

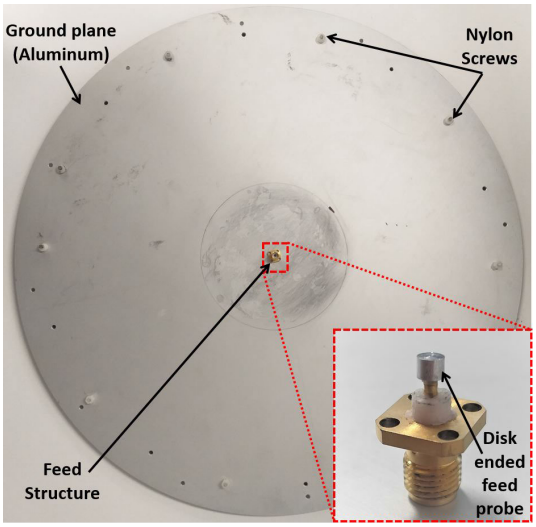

(b)

FIGURE 6. Fabricated prototype of the CP RLSA antenna; (a) Front view, (b) Back view.

B. INPUT MATCHING

The magnitude of the input refection coefficient $|S_{11}|$, measured using an Agilent PNA-X N5242A vector network analyzer, is plotted in Fig. 7. The magnitude of reflection coefficient is less than -10 dB in the measured frequency range from 19 GHz to 21 GHz. This CP RLSA antenna has a return loss bandwidth greater than 10%.

C. NEAR-FIELD DISTRIBUTION

The numerical simulation data was post processed to extract relevant amplitude and the phase distributions of the electric field at the operating frequency of 20 GHz, which are shown in Figure 8. The electric near-field patterns of E_x and E_y are taken in the XZ plane extending from the top surface of the antenna to a distance of $1\lambda_0$ (15 mm above the radiating plate). The figure shows a radial taper amplitude

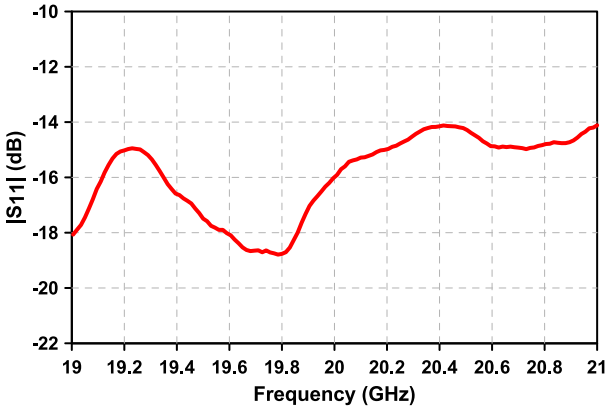

FIGURE 7. Measured reflection coefficient magnitude $|S_{11}|$ of the antenna prototype.

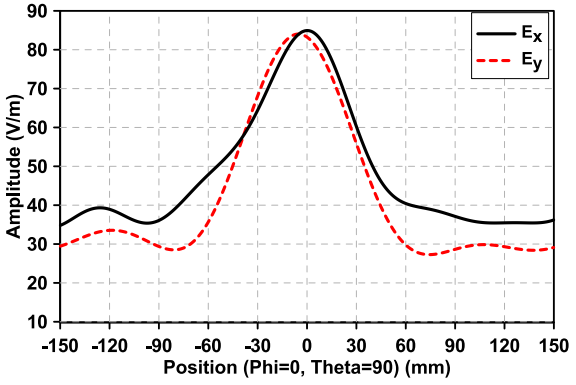

FIGURE 8. Near-field amplitude distribution of the antenna at a distance of $1\lambda_0$.

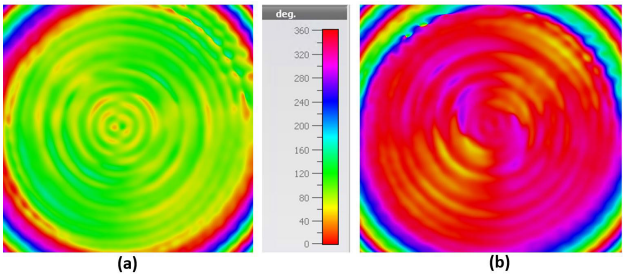

FIGURE 9. Antenna near-field phase distribution at 20 GHz on a plane that is $1\lambda_0$ above the radiating aperture; (a) E_x component, (b) E_y component.

distribution. 2D and 1D views of the near-field phase distribution of the antenna at 20 GHz are shown in Figure 9 and Figure 10, respectively. It is evident from the phase distribution that antenna radiates nearly planar and symmetric phase fronts, demonstrating the uniformity in the aperture phase distribution.

D. GAIN, AXIAL RATIO AND EFFICIENCY

The far-field patterns were measrued in an NSI near-field spherical antenna range. The gain was measured using the gain comparison method with a WR-51 standard gain horn. The antenna beam peak is in the boresight direction. The

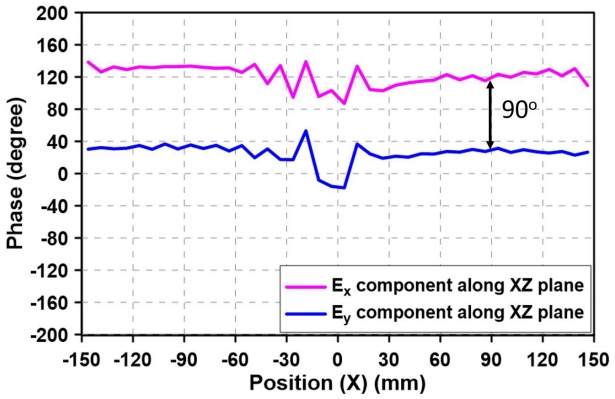

FIGURE 10. Near-field phase distribution of the antenna at a distance of $1\lambda_0$ above the radiating plate. 90° phase difference between E_x and E_y is noted.

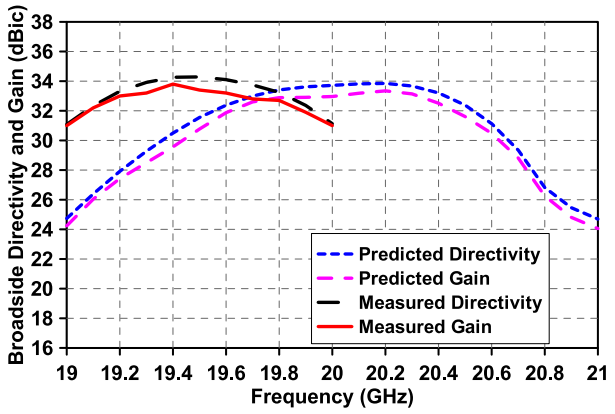

FIGURE 11. Predicted and measured boresight directivity and gain.

measured peak gain and directivity in the frequency range from 19 GHz to 21 GHz are plotted in Fig. 11. The predicted gain and directivity are also included in the same figure. The predicted peak directivity is 33.8 dBic and predicted peak gain is 33 dBic at 20 GHz. The predicted 3dB gain bandwidth is 6%, from 19.4 GHz to 20.6 GHz. The measured peak directivity is 34.3 dBic and measured peak gain is 33.8 dBic at 19.4 GHz. Here, one can observe a 3% frequency shift toward lower frequencies in the measured results. This shift can be attributed to manufacturing tolerances of the parts and components used in assembling the prototype. The antenna has a measured 3dB gain bandwidth of 5.4%, which extends from 18.95 GHz to 20 GHz.

The predicted and measured axial ratio of the antenna is shown in Figure 12. The axial ratio is less than 3dB, satisfying the standard circular polarization condition, and the 3dB axial ratio bandwidth is more than 5%. Better than expected results obtained in axial ratio measurements are due to fabrication tolerances. The measured aperture efficiency of the prototype is 48%. The radiation efficiency is 94.2% at 20 GHz. Note that in this design no absorber is used, therefore the losses are very low, and efficiency is excellent. The overall efficiency varies between 82% to 92% in the frequency band from 19 GHz to 21 GHz.

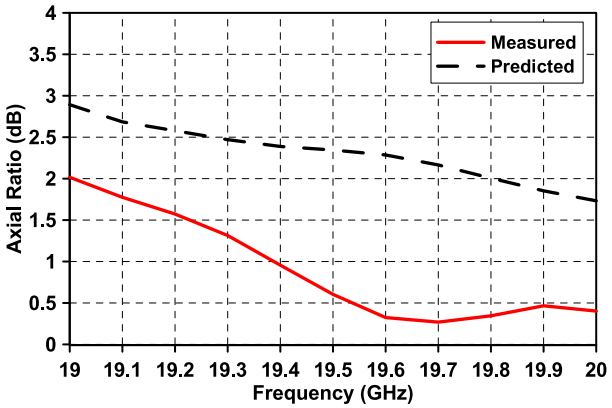

FIGURE 12. Boresight axial ratio of the fabricated prototype.

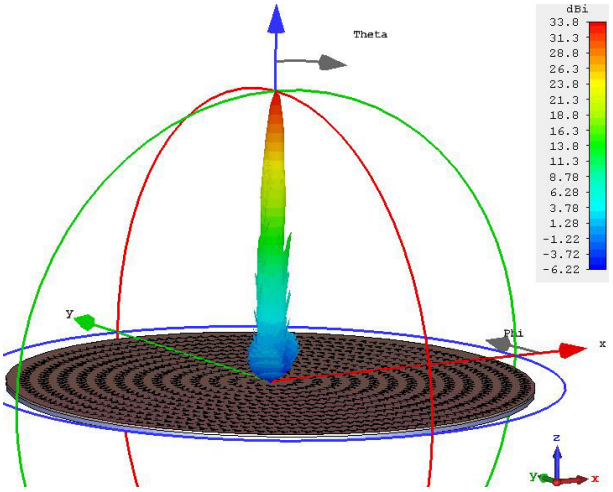

FIGURE 13. 3D view of the radiation pattern at 20 GHz.

E. RADIATION PATTERNS

The antenna has stable radiation patterns in the measured frequency band. The radiation pattern measurements were carried out in a NSI spherical near-field range at AusAMF. The predicted 3D radiation pattern at 20 GHz is shown in Fig. 13. The cross-polar level at 20 GHz is 20.5 dB below the co-polar level in the boresight direction. The predicted radiation patterns of the antenna, on $\phi = 0°$ plane and $\phi = 90°$ plane, are plotted in Fig. 14 at six frequencies within the gain bandwidth. These patterns clearly show directive beams pointing towards boresight with significantly low side lobe levels. It can be seen that the SLLs in both $\phi = 0°$ and $\phi = 90°$ planes remain below -20 dB. Antenna performance figures for the given six frequencies are summarized in Table 4.

The measured radiation patterns at four different frequencies, on $\phi = 90°$ plane and $\phi = 0°$ plane, respectively, are shown in Fig. 15 and Fig. 16 along with the radiation pattern envelopes (RPE) of Class-1 and Class-2 antennas, as specified by ETSI. It is evident from the figures that the prototype has good radiation pattern qualities with significantly lower SLLs and have met the requirements of the envelope specified for ETSI Class-1 and Class-2 antennas except for the angles over 75° on $\phi = 0°$ plane, where the measured pattern exceeded Class-2 RPE.

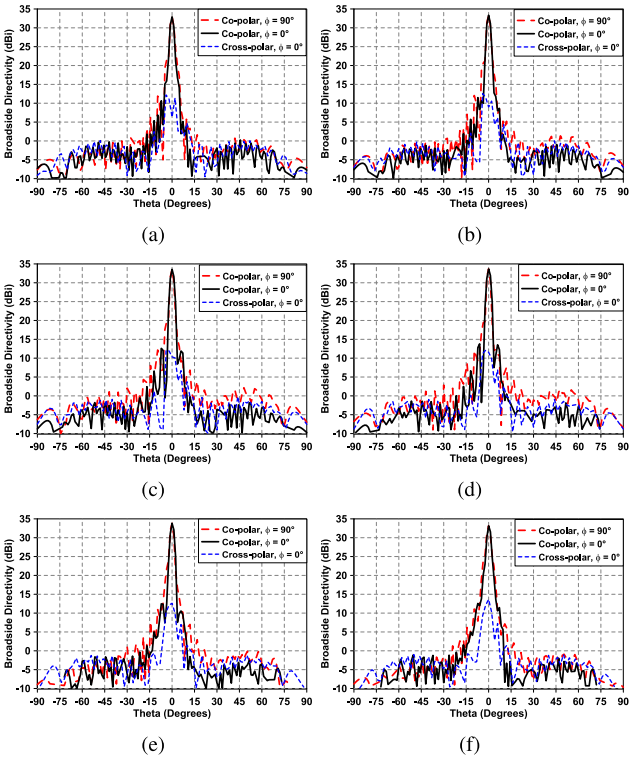

FIGURE 14. Radiation patterns of the antenna on $\phi = 0°$ and $\phi = 90°$ planes; (a) 19.7 GHz, (b) 19.8 GHz, (c) 19.9 GHz, (d) 20 GHz, (e) 20.2 GHz, (f) 20.4 GHz.

TABLE 4. Performance figures of the CP RLSA at six different frequencies.

Frequency (GHz)	19.7	19.8	19.9	20	20.2	20.4
Gain (dBic)	32.6	32.9	32.9	33	33.2	32.5
SLL ($\phi = 0°$) dB	-22.3	-21.9	-21	-20.2	-21.3	-20.6
SLL ($\phi = 90°$) dB	-21	-21.3	-21.4	-21.3	-22.9	-22.1
θ_{3dB} ($\phi = 0°$) degrees	2.6	2.6	2.7	2.7	2.7	2.6
θ_{3dB} ($\phi = 90°$) degrees	2.6	2.5	2.4	2.4	2.5	2.7
Radiation Efficiency (%)	94.2	94.5	94.2	93.8	94	94

F. DISCUSSION

Table 5 lists the performance figures of the prototyped CP RLSA and compares with some previously published RLSA antennas. As it can be seen from the table that the proposed CP RLSA antenna has the lowest side lobe levels and highest antenna efficiency compared to the previously reported RLSAs. Antenna efficiency is high because no absorber was used in this design. The new antenna also has

TABLE 5. Comparison of the proposed CP RLSA with conventional RLSAs.

Ref	Frequency	Antenna size (diameters)	10dB return loss bandwidth	Polarization	Axial ratio	Gain	Side lobe level	3dB gain bandwidth	Overall antenna efficiency	Antenna thickness	Absorber	Gain BW product	Area	Gain BW product/ Area
	GHz	λ_0	%		dB	dBi	dB	%	%	λ_0		GBP	λ_0^2	GBP/ A
[41]	12	16	2.5	CP	0.5	32	-11	2.5	62.8	3.2	Yes	3,962.2	200.9	19.7
[42]	9.27	15.8	5.3	LP	N/A	31.3	-13	2.5	54	3	Yes	3,372.4	195.9	17.2
[39]	9.42	17	1	CP	1.6	29	-7	1	44.8	4.3	Yes	794.3	226.8	3.5
[10]	16.9	20.1	2.1	LP	N/A	33	-11	3.5	54	0.51	Yes	6,983.4	317.1	22
[36]	22	22	-	CP	-	34.5	-11	4.6	54	0.22	Yes	12,964.5	379.9	34.1
[37]	11.6	16	8.3	LP	N/A	30.4	-15	-	48	0.34	Yes	-	200.9	-
[38]	12	24	4.2	CP	1	35.4	-10	2.5	65	0.36	Yes	8,668.4	452.1	19.1
[40]	13.7	11.6	8.8	CP	-	18.2	-15	-	58.7	-	Yes	-	105.6	-
[23]	12	16	4.2	CP	1	32.5	-15	4.1	75	0.35	Yes	7,290.9	200.9	36.2
[8]	12.5	25	12.2	LP	N/A	31	-14	4.8	57	0.3	Yes	6,042.8	490.6	12.3
This work	20	23	>10	CP	0.4	33	> -20	5.4	84.4	0.3	No	10,774.4	415.2	25.9

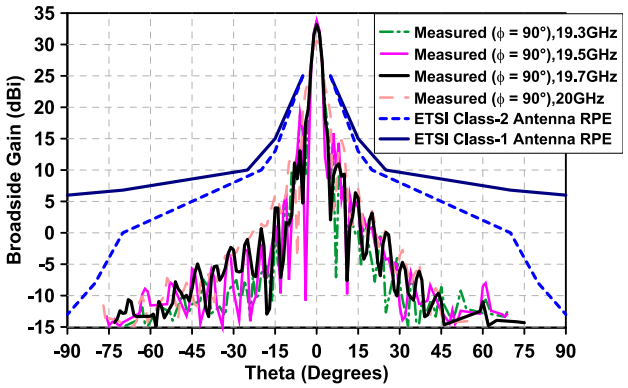

FIGURE 15. Measured radiation patterns of the antenna at $\phi = 90°$ plane. ETSI Class-1 and Class-2 RPEs are also shown.

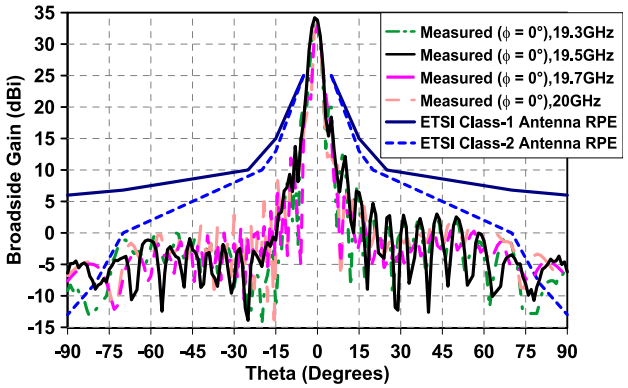

FIGURE 16. Measured radiation patterns of the antenna at $\phi = 0°$ plane. ETSI Class-1 and Class-2 RPEs are also shown.

a larger measured 3dB gain bandwidth compared to the previous RLSAs. Furthermore, the height of the new CP RLSA antenna is the second lowest in terms of wavelengths at the center frequency.

V. CONCLUSION

In this paper, we demonstrated a method to control the near-field amplitude distribution of CP RLSA antennas to improve far-field performance while making the near-field phase distribution nearly uniform. The tapered amplitude distribution was achieved using a slot coupling analysis. This method relies on the fact that the energy coupled by a radiating slot to space depends on slot length and internal field strength, and by changing slot lengths on the radiating surface, different near-field amplitude distributions can be achieved. The measured prototype, which is 4.6 mm ($0.3\lambda_0$) thick, has a peak gain of 33.8 dBic, an improved 3dB gain bandwidth of 5.4%, a return loss bandwidth of more than 10% and total antenna efficiency of 84.4%. Measurement results have shown that by using the proposed strategy, amplitude distribution can be controlled, which leads to significant reduction in side lobe levels. At 20 GHz, the side lobe levels of the measured prototypes are less than -20 dB.

REFERENCES

[1] M. Ando, K. Sakurai, N. Goto, K. Arimura, and Y. Ito, "A radial line slot antenna for 12 GHz satellite TV reception," *IEEE Trans. Antennas Propag.*, vol. 33, no. 12, pp. 1347–1353, Dec. 1985.

[2] P. W. Davis and M. E. Bialkowski, "Linearly polarized radial-line slot-array antennas with improved return-loss performance," *IEEE Antennas Propag. Mag.*, vol. 41, no. 1, pp. 52–61, Feb. 1999.

[3] J. Warshowsky, C. Kulisan, and D. Vail, "20 GHz phased array antenna for GEO satellite communications," in *Proc. 21st Century Mil. Commun. Architectures Technol. Inf. Superiority (MILCOM)*, vol. 2, 2000, pp. 1187–1191.

[4] M. U. Afzal and K. P. Esselle, "Steering the beam of medium-to-high gain antennas using near-field phase transformation," *IEEE Trans. Antennas Propag.*, vol. 65, no. 4, pp. 1680–1690, Apr. 2017.

[5] A. A. Baba, R. M. Hashmi, K. P. Esselle, M. Attygalle, and D. Borg, "A millimeter-wave antenna system for wideband 2-D beam steering," *IEEE Trans. Antennas Propag.*, vol. 68, no. 5, pp. 3453–3464, May 2020.

[6] K. Singh, M. U. Afzal, M. Kovaleva, and K. P. Esselle, "Controlling the most significant grating lobes in two-dimensional beam-steering systems with phase-gradient metasurfaces," *IEEE Trans. Antennas Propag.*, vol. 68, no. 3, pp. 1389–1401, Mar. 2020.

[7] M. N. Y. Koli, M. U. Afzal, K. P. Esselle, and R. M. Hashmi, "An all-metal high-gain radial-line slot-array antenna for low-cost satellite communication systems," *IEEE Access*, vol. 8, pp. 139422–139432, 2020.
[8] P. W. Davis and M. E. Bialkowski, "Experimental investigations into a linearly polarized radial slot antenna for DBS TV in Australia," *IEEE Trans. Antennas Propag.*, vol. 45, no. 7, pp. 1123–1129, Jul. 1997.
[9] S. I. Zakwoi, T. A. Rahman, I. Maina, and O. Elijah, "Design of ka band downlink radial line slot array antenna for direct broadcast satellite services," in *Proc. IEEE Asia–Pacific Conf. Appl. Electromagn. (APACE)*, Dec. 2014, pp. 159–162.
[10] A. Mazzinghi, M. Albani, and A. Freni, "Double-spiral linearly polarized RLSA," *IEEE Trans. Antennas Propag.*, vol. 62, no. 9, pp. 4900–4903, Sep. 2014.
[11] J. Suryana and D. B. Kusuma, "Design and implementation of RSLA antenna for mobile DBS application in ku-band downlink direction," in *Proc. Int. Conf. Electr. Eng. Informat. (ICEEI)*, Aug. 2015, pp. 341–345.
[12] N. Y. Koli, M. U. Afzal, K. P. Esselle, and M. Z. Islam, "Comparison between fully and partially filled dielectric materials on the waveguide of circularly polarised radial line slot array antennas," in *Proc. Int. Workshop Antenna Technol. (iWAT)*, Feb. 2020, pp. 1–3.
[13] T. Purnamirza, T. A. Rahman, and M. H. Jamaluddin, "The extreme beamsquint technique to minimize the reflection coefficient of very small aperture radial line slot array antennas," *J. Electromagn. Waves Appl.*, vol. 26, pp. 17–18, Dec. 2012.
[14] M. I. Imran, A. R. Tharek, and A. Hasnain, "An optimization of beam squinted radial line slot array antenna design at 5.8 GHz," in *Proc. IEEE Int. RF Microw. Conf.*, Dec. 2008, pp. 139–142.
[15] M. I. Imran, A. Riduan, A. R. Tharek, and A. Hasnain, "Beam squinted radial line slot array antenna (RLSA) design for point-to-point WLAN application," in *Proc. Asia–Pacific Conf. Appl. Electromagn.*, Dec. 2007, pp. 1–4.
[16] K. Kelly and F. Goebels, "Annular slot monopulse antenna arrays," *IEEE Trans. Antennas Propag.*, vol. 12, no. 4, pp. 391–403, Jul. 1964.
[17] T. Nguyen, K. Sakurai, J. Hirokawa, M. Ando, O. Amano, S. Koreeda, T. Matsuzaki, and Y. Kamata, "A concise design of large mm-wave radial line slot antenna with honeycomb structures for space application," in *Proc. 31st URSI Gen. Assem. Sci. Symp. (URSI GASS)*, Aug. 2014, pp. 1–4.
[18] N. Y. Koli, M. U. Afzal, K. P. Esselle, and M. Z. Islam, "A radial line slot array antenna with improved radiation patterns for satellite communication," in *2019 13th Eur. Conf. Antennas Propag. (EuCAP)*, 2019, pp. 1–2.
[19] M. Ando, "New DBS receiver antennas," in *Proc. 23rd Eur. Microw. Conf.*, Oct. 1993, pp. 84–92.
[20] M. Ando, K. Sakurai, and N. Goto, "Characteristics of a radial line slot antenna for 12 GHz band satellite TV reception," *IEEE Trans. Antennas Propag.*, vol. 34, no. 10, pp. 1269–1272, Oct. 1986.
[21] M. Ando, T. Numata, J.-I. Takada, and N. Goto, "A linearly polarized radial line slot antenna," *IEEE Trans. Antennas Propag.*, vol. 36, no. 12, pp. 1675–1680, Dec. 1988.
[22] M. E. Bialkowski and P. W. Davis, "Analysis of a circular patch antenna radiating in a parallel-plate radial guide," *IEEE Trans. Antennas Propag.*, vol. 50, no. 2, pp. 180–187, Feb. 2002.
[23] M. Takahashi, J. Takada, M. Ando, and N. Goto, "Characteristics of small-aperture, single-layered, radial-line slot antennas," *IEE Proc. H, Microw., Antennas Propag.*, vol. 139, no. 1, pp. 79–83, Feb. 1992.
[24] I. M. Ibrahim, T. A. Rahman, M. I. Sabran, and M. F. Jamlos, "Bandwidth enhancement through slot design on RLSA performance," in *Proc. IEEE REGION Symp.*, Apr. 2014, pp. 228–231.
[25] N. Y. Koli, M. U. Afzal, K. P. Esselle, R. M. Hashmi, M. Z. Islam, and S. Shrestha, "A double layer circularly polarised radial line slot array antenna with uniform aperture illumination," in *Proc. 4th Austral. Microw. Symp. (AMS)*, Feb. 2020, pp. 1–2.
[26] M. Takahashi, M. Ando, N. Goto, Y. Numano, M. Suzuki, Y. Okazaki, and T. Yoshimoto, "Dual circularly polarized radial line slot antennas," *IEEE Trans. Antennas Propag.*, vol. 43, no. 8, pp. 874–876, Aug. 1995.
[27] Y. Liu, H. Xiao, and G. Lu, "Design of a high gain circular polarized radial line slot antenna," in *Proc. 7th Int. Symp. Comput. Intell. Design*, Dec. 2014, pp. 490–493.
[28] P. W. Davis, "A linearly polarised radial line slot array antenna for direct broadcast satellite services," Ph.D. dissertation, School Inf. Technol. Elect. Eng., Univ. Queensland, Brisbane, QLD, Australia, 2000.
[29] M. N. Y. Koli, M. U. Afzal, K. Esselle, and M. Z. Islam, "A high gain radial line slot array antenna for satellite reception," in *Proc. Austral. Microw. Symp. (AMS)*, Feb. 2018, pp. 65–66.
[30] S. Z. Iliya, T. A. Rahman, H. U. Iddi, T. Purnamirza, S. I. Orakwue, and O. Elijah, "Optimization of radial line slots array antenna design for satellite communications," in *Proc. IEEE Int. Conf. Space Sci. Commun. (IconSpace)*, Jul. 2013, pp. 45–50.
[31] J. M. F. Gonzalez, P. Padilla, G. Exposito-Dominguez, and M. Sierra-Castaner, "Lightweight portable planar slot array antenna for satellite communications in X-band," *IEEE Antennas Wireless Propag. Lett.*, vol. 10, pp. 1409–1412, 2011.
[32] S. Zagriatski and M. E. Bialkowski, "Circularly polarised radial line slot array antenna for wireless LAN access point," in *Proc. 15th Int. Conf. Microw., Radar Wireless Commun.*, vol. 2, May 2004, pp. 649–652.
[33] J. I. Herranz-Herruzo, A. Valero-Nogueira, E. Alfonso, and V. M. Rodrigo, "Linearly-polarized radial-line slot-dipole array antenna without canceling elements," in *Proc. IEEE Antennas Propag. Soc. Int. Symp.*, Jun. 2007, pp. 4296–4299.
[34] T. Purnamirza, D. Kristanto, and M. I. Ibrahim, "A design of compact radial line slot array (RLSA) antennas for Wi-Fi market needs," *Prog. Electromagn. Res. Lett.*, vol. 64, pp. 21–28, Jan. 2016.
[35] J. I. Herranz, A. Valero-Nogueira, F. Vico, and V. M. Rodrigo, "Optimization of beam-tilted linearly polarized radial-line slot-array antennas," *IEEE Antennas Wireless Propag. Lett.*, vol. 9, pp. 1165–1168, 2010.
[36] M. Albani, A. Mazzinghi, and A. Freni, "Automatic design of CP-RLSA antennas," *IEEE Trans. Antennas Propag.*, vol. 60, no. 12, pp. 5538–5547, Dec. 2012.
[37] J. Takada, M. Ando, and N. Goto, "A reflection cancelling slot set in a linearly polarized radial line slot antenna," *IEEE Trans. Antennas Propag.*, vol. 40, no. 4, pp. 433–438, Apr. 1992.
[38] M. Takahashi, J.-I. Takada, M. Ando, and N. Goto, "A slot design for uniform aperture field distribution in single-layered radial line slot antennas," *IEEE Trans. Antennas Propag.*, vol. 39, no. 7, pp. 954–959, Jul. 1991.
[39] C.-W. Yuan, S.-R. Peng, T. Shu, Z.-Q. Li, and H. Wang, "Designs and experiments of a novel radial line slot antenna for high-power microwave application," *IEEE Trans. Antennas Propag.*, vol. 61, no. 10, pp. 4940–4946, Oct. 2013.
[40] M. Sierra-Castaner, M. Sierra-Perez, M. Vera-Isasa, and J. L. Fernandez-Jambrina, "Low-cost monopulse radial line slot antenna," *IEEE Trans. Antennas Propag.*, vol. 51, no. 2, pp. 256–263, Feb. 2003.
[41] S. Peng, C.-W. Yuan, T. Shu, J. Ju, and Q. Zhang, "Design of a concentric array radial line slot antenna for high-power microwave application," *IEEE Trans. Plasma Sci.*, vol. 43, no. 10, pp. 3527–3529, Oct. 2015.
[42] S. Peng, C. Yuan, T. Shu, and X. Zhao, "Linearly polarised radial line slot antenna for high-power microwave application," *IET Microw., Antennas Propag.*, vol. 11, no. 5, pp. 680–684, Apr. 2017.
[43] Y. Wang, H. Xiao, G. Lu, J. Lin, and T. Li, "The investigation for a circularly polarized radial line slot antenna with low side lobes and high gain," in *Proc. Int. Conf. Microw. Millim. Wave Technol. (ICMMT)*, vol. 3, May 2012, pp. 1–2.
[44] I. Maina, T. A. Rahman, and M. Khalily, "Bandwidth enhanced and sidelobes level reduced radial line slot array antenna at 28 GHz for 5G next generation mobile communication," *ARPN J. Eng. Appl. Sci.*, vol. 10, pp. 5752–5757, 2015.
[45] A. Balanis, *Antenna Theory: Analysis and Design*. Hoboken, NJ, USA: Wiley, 2016.

MST NISHAT YASMIN KOLI (Graduate Student Member, IEEE) received the B.S. degree in electronics and telecommunication engineering from the Rajshahi University of Engineering and Technology (RUET), Rajshahi, Bangladesh, in 2015, and the M.Res. degree in electronics engineering from Macquarie University, Sydney, NSW, Australia, in 2017, where she is currently pursuing the Ph.D. degree with the Centre for Collaboration in Electromagnetic and Antenna Engineering (CELANE).

From 2015 to 2016, she was a Lecturer with the Electrical and Electronics Engineering Department, European University, Dhaka, Bangladesh. Her research interests include antenna array, high-gain planar metasurface based antennas, radial-line slot array antennas, beam steering metasurfaces, antennas for radio astronomy and satellite communication, and microwave and millimetre-wave antennas. She received several prestigious awards, including the International Research Training Program Scholarship (iRTP) for the MRes and International Macquarie University Research Excellence Scholarship (iMQRES) for her Ph.D. degree.

MUHAMAMD U. AFZAL (Senior Member, IEEE) received the bachelor's degree (Hons.) in electronics engineering and the master's degree in computational science and engineering from the National University of Sciences and Technology (NUST), Islamabad, in 2009 and 2011, respectively, and the Ph.D. degree in electronics engineering from Macquarie University, Australia, in 2017.

In 2010, he started his professional career as a Lab Engineer at the Research Institute for Microwave and Millimetre-Wave Studies (RIMMS) NUST, Islamabad. In 2012, he was promoted to the position of Lecturer, which he continued till February 2013. In 2017, after his Ph.D., he was offered a postdoctoral position for three years on a project funded by the Australian Research Council (ARC) through the Discovery Grant Scheme at Macquarie University. Apart from the project-specific research, he has co-supervised one Ph.D., three master's of research, and several undergraduate thesis students at Macquarie University. He is currently a Research Fellow with the University of Technology Sydney. He developed the concept of near-field phase transformation during his doctorate research, which was demonstrated to enhance the directivity of low-gain aperture antennas in the IEEE TAP paper entitled ''Dielectric phase-correcting structures for electromagnetic band-gap resonator antennas.'' He is the co-inventor of efficient antenna beam-steering technology referred to as Near-Field Meta-Steering. This technology received the ''Highly Commended'' certificate in the Five Future-Shaping Research Priorities category in the 2017 Academic Staff Awards at Macquarie University. To commercialize the outcomes of his research, he led a team of colleagues in a CSIRO-sponsored ON Prime 2 in 2017—a pre-accelerator program designed to commercialize outcomes of academic research in Australia.

Dr. Afzal has received several awards and scholarships, including a merit-based scholarship in six out of eight semesters during the undergraduate degree, a scholarship of complete fee waiver during the postgraduate degree, and the international Macquarie Research Excellence (iMQRES) scholarship towards Doctorate study from Macquarie University. He received a competitive travel grant in 2015 to present my research work at a flagship conference under the Antennas and Propagation Society (APS) in Vancouver, Canada. He assisted in preparing several grant applications, including a successful ARC Discovery Grant in 2018. He was third CI in a team of five who received a grant of more than $20K from the German Academic Exchange Service in a funding scheme ''Australia-Germany Joint Research Co-Operation Scheme.'' He is currently working on the development of satellite-terminal antenna technology and has research interests in electromagnetic phase-shifting structures, frequency selective surfaces, and similar metamaterials for microwave and millimeter-wave antenna applications.

KARU P. ESSELLE (Fellow, IEEE) received the B.Sc. degree (Hons.) in electronic and telecommunication engineering from the University of Moratuwa, Sri Lanka, and the M.A.Sc. and Ph.D. degrees with near-perfect GPA in electrical engineering from the University of Ottawa, Canada.

He was the Director of the WiMed Research Centre and Associate Dean—Higher Degree Research (HDR) of the Division of Information and Communication Sciences and directed the Centre for Collaboration in Electromagnetic and Antenna Engineering, Macquarie University. He is currently the Distinguished Professor in Electromagnetic and Antenna Engineering at the University of Technology Sydney and a Visiting Professor of Macquarie University, Sydney. According to 2019 Special Report on Research published by The Australian national newspaper, he is the National Research Field Leader in Australia in both Microelectronics and Electromagnetisms fields. He has authored approximately 600 research publications and his papers have been cited over 10,000 times. In 2019 , his publications received 1,200 citations. He is the first Australian Antenna Researcher ever to reach Google Scholar h-index of 30 and his citation indices have been among the top Australian antenna researchers for a long time (at present: i10 is 181 and h-index is 49). Since 2002, his research team has been involved with research grants, contracts, and Ph.D. scholarships worth about 20 million dollars, including 15 Australian Research Council grants, without counting the 245 million-dollar SmartSat Corporative Research Centre, which started in 2019. His research has been supported by many national and international organizations, including Australian Research Council, Intel, US Air Force, Cisco Systems, Hewlett-Packard, Australian Department of Defense, Australian Department of industry, and German and Indian governments. He has provided expert assistance to more than a dozen companies including Intel, Hewlett Packard Laboratory (USA), Cisco Systems (USA), Audacy (USA), Cochlear, Optus, ResMed and Katherine-Werke (Germany). His team designed the high-gain antenna system for the world's first entirely Ka-band CubeSat made by Audacy, Mountain View, CA, USA, and launched to space by SpaceX in December 2018. This is believed to be the first Australian-designed high-gain antenna system launched to space, since CSIRO-designed antennas in Australia's own FedSat launched in 2002. He is in the College of Expert Reviewers of the European Science Foundation (2019–2022) and he has been invited to serve as an international expert/research grant assessor by several other research funding bodies as well, including the European Research Council and funding agencies in Norway, Belgium, The Netherlands, Canada, Finland, Hong-Kong, Georgia, South Africa, and Chile. He has been invited by Vice-Chancellors of Australian and overseas universities to assess applications for promotion to professorial levels. He has also been invited to assess grant applications submitted to Australia's most prestigious schemes such as Australian Federation Fellowships and Australian Laureate Fellowships. In addition to a large number of invited conference speeches he has given, he has been an invited plenary/extended/keynote speaker of several IEEE and other conferences and workshops, including EuCAP 2020 Copenhagen, Denmark; URSI'19 Seville, Spain; and 23rd ICECOM 2019, Dubrovnik, Croatia.

Dr. Esselle has also served as a member of the Dean's Advisory Council and the Division Executive and as the Head of the Department several times. He is a Fellow of the Royal Society of New South Wales and Engineers Australia. His awards include one of the two finalists for the 2020 Australian Eureka Prize for Outstanding Mentor of Young Researchers; the 2019 Motohisa Kanda Award (from the IEEE USA) for the most cited paper in the IEEE Transactions on EMC in the past five years; the 2019 Macquarie University Research Excellence Award for Innovative Technologies; the 2019 ARC Discovery International Award; the 2017 Excellence in Research Award from the Faculty of Science and Engineering; the 2017 Engineering Excellence Award for Best Innovation; the 2017 Highly Commended Research Excellence Award from Macquarie University; the 2017 Certificate of Recognition from the IEEE Region 10; the 2016 and 2012 Engineering Excellence Awards for Best Published Paper from IESL NSW Chapter; the 2011 Outstanding Branch Counselor Award from the IEEE headquarters (USA); and the 2009 Vice Chancellor's Award for Excellence in Higher Degree Research Supervision and 2004 Innovation Award for Best Invention Disclosure. His mentees have been awarded many fellowships, awards, and prizes for their research achievements. Fifty-three international experts who examined the theses of his Ph.D. graduates ranked them in the top 5% or 10%. Two of his recent students were awarded Ph.D. with the highest honour at Macquarie University—the Vice Chancellor's Commendation. Since 2018, he has been chairing the prestigious Distinguished Lecturer Program Committee of the IEEE Antennas and Propagation (AP) Society—the premier global learned society dedicated for antennas and propagation, which has close to 10,000 members worldwide. After two stages in the selection process, he was also selected by this Society as one of two candidates in the ballot for 2019 President of the Society. Only three people from Asia or Pacific apparently have received this honour in the 68-year history of this Society. He is also one of the three Distinguished Lecturers (DL) selected by the Society in 2016. He is the only Australian to chair the AP DL Program ever, the only Australian AP DL in almost two decades, and second Australian AP DL ever (after UTS Distinguished Visiting Professor Trevor Bird). He has been continuously serving the IEEE AP Society Administrative Committee in several elected or ex-officio positions since 2015. He is also the Chair of the Board

of Management of the Australian Antenna Measurement Facility, and was the elected Chair of both the IEEE New South Wales (NSW), and the IEEE NSW AP/MTT Chapter, in 2016 and 2017, respectively. He is an Associate Editor of the IEEE TRANSACTIONS ON ANTENNAS PROPAGATION, *IEEE Antennas and Propagation Magazine*, and IEEE ACCESS. He is the Track Chair pf IEEE AP-S 2020 Montreal, Technical Program Committee Co-Chair of ISAP 2015, APMC 2011, and TENCON 2013, and the Publicity Chair of ICEAA/IEEE APWC 2016, IWAT 2014, and APMC 2000. His research activities are posted in the web at http://web.science.mq.edu.au/ esselle/ and https://www.uts.edu.au/staff/karu.esselle.

RAHEEL M. HASHMI (Member, IEEE) received the B.S. degree (Hons. Class I) from CIIT, Pakistan, the M.S. degree from the Politecnico di Milano, Italy, and the Ph.D. degree from Macquarie University, Australia.

From 2012 to 2015, he was a Visiting Researcher with the CSIRO Astronomy and Space Science Division, Australia. His research interests are in novel antenna technologies and microwave/millimeter-wave devices for applications in communications sector, defence, and smart living. He is currently a Senior Lecturer within the Faculty of Science and Engineering, Macquarie University, Australia. His research explores the electromagnetic response of artificially engineered materials, using them to manipulate electromagnetic radiation for creating simple, yet highly efficient antennas and wireless components. He has received over 1.6 million dollars worth of research grants, contracts, and fellowships. He has contributed over 80 peer-reviewed journal and conference papers, two scholarly book chapters, and is an inventor on two patent applications.

Dr. Hashmi was a recipient of several prestigious awards and fellowships, including the 2017 Young Scientist Award (Field and Waves) from the International Union of Radio Science (URSI), the 2012 Commonwealth IPRS Award, the CSIRO OCE Ph.D. Fellowship, and the Institute's Gold Medal from the CIIT, Pakistan. He was the Chair of the IEEE Antennas and Propagation/Microwave Theory and Techniques Joint Chapter (2018–2019) and the Vice Chair of the IEEE Young Professionals Affinity Group in New South Walesuring (2017–2018). He regularly reviews for several top journals and conferences in his field, including the IEEE TRANSACTIONS ON ANTENNAS AND PROPAGATION, IEEE ANTENNAS AND WIRELESS PROPAGATION LETTERS, IEEE ACCESS, Asia–Pacific Microwave Conference, International Conference on Electromagnetics in Advanced Applications, AP-S Symposium, and EuCAP. He serves as an Associate Editor for the *IET Microwaves, Antennas and Propagation*, and as a Guest Editor for IEEE ACCESS and *Microwave and Optical Technology Letters* (Wiley).